Available online at www.sciencedirect.com
SCIENCE DIRECT
Polymer 47 (2006) 4454–4460
polymer
www.elsevier.com/locate/polymer

Study of surface conditions and shear flow of LCP melts in nanochannels through molecular dynamics simulation

Kai Leung Yung [a], Lan He [b,*], Yan Xu [a], Yun Wen Shen [b]

[a] Department of Industrial and Systems Engineering, The Hong Kong Polytechnic University, Hung Hom, Kowloon, Hong Kong, China
[b] Northwestern Polytechnical University, MailBox 178, Xi'An 710072, China

Received 26 January 2006; received in revised form 8 April 2006; accepted 10 April 2006

Abstract

The rheological properties and phase orientation of liquid crystalline polymer (LCP) melts flowing in a nanochannel with different surface roughness are investigated by molecular dynamics (MD) simulations. The molecular chains of LCPs are depicted by a newly developed molecular model named GB-spring-bead model, which has proved to be efficient and accurate in studying the phase transition behaviors of semi-flexible main chain LCPs [Yung KL, He L, Xu Y, Shen YW. Polymer 2005;46:11881 [1]]. The surfaces are modeled as rough atomic serrated walls whereby the roughness is characterized by the period and amplitude of serrations. Simulation results have shown that the surface roughness affects greatly the rheological properties and phase orientations of LCP melts in a nanochannel (the distance between the upper wall and the lower wall is 12.8 nm). As the amplitude of serration increases, the shear viscosity of LCP increases nonlinearly while its orientational order parameter decreases. When the serration amplitude reaches a certain magnitude, a phase transition (from nematic to isotropic phase) happens, which increases the viscosity of the nano LCP flow drastically. On the other hand, the influence of serration period on the shear viscosity and orientational order parameter is not so obvious relatively. Findings in this study provide very useful information in the injection molding of plastic products with nanofeatures.

Keywords: Liquid crystalline polymers; GB-spring-bead model; Molecular dynamics simulations

1. Introduction

LCPs are a new class of macromolecular materials that, suitably processed, behave in a self-reinforcing manner and exhibit special properties, such as lower viscosity at certain range of temperature, in comparison with tranditional polymers. In a certain processing condition, LCP molecules show liquid crystalline features where their rigid units are aligned in the same direction. When LCPs are in liquid crystalline phase, their viscosities will be remarkably low. Due to the good flowability and high mechanical performance, such as extra high stiffness in solid state, LCPs have become one of the most promising materials in developing micro and nano components. However, there are still many difficulties in processing thermotropic LCPs into micro and nano components through injection molding such as how to optimize the processing conditions to obtain an optimum orientational distribution in the LCP melt during the mold filling process. In the last decades, a number of investigators [2–5] examined how the injection pressure and rate affected the mechanical properties of injection molded specimens made from LCPs at macro scale. They concluded that the tensile modulus and strength were better when the product was formed at lower value of injection pressure and injection speed. It is also found that temperature of mould and roughnesses of mould wall are important factors influencing the micro/nano LCP melt flow and the mechanical properties of specimens. However, to predict and understand how and why these processing conditions affect the nano LCP flow is a difficult task even using molecular dynamics simulation, since LCP melt flows are more complex than other polymeric flows. Firstly, there are phase transitions in LCP melts, which demands larger number of data and very long calculation time. Secondly, there is intrinsic anisotropy in the liquid crystalline state, which requires the simulation program not only being able to simulate movements of molecules accurately but also can perform large scale investigations efficiently. Recent literatures [6–8] show existing molecular models have limitations in studying nano flow of LCP melts on large size. For instance, although being

* Corresponding author. Tel.: +852 27666312; fax: +852 23625267.
E-mail address: npusujie@126.com (L. He).

0032-3861/$ - see front matter © 2006 Elsevier Ltd. All rights reserved.
doi:10.1016/j.polymer.2006.04.028

accurate in describing movements of LCP molecular chains, Gay-Berne(GB)/Lennard-Jones(LJ) model needs very long computational time, which is unbearable for computing large amount of molecules for forming collective phenomena. The bead-spring model, although being much more efficient, fails to describe detailed molecular features of LCPs (such as unable to describe the odd–even effect), which curtails the accuracy of simulations. Consequently, there are very few studies on simulating the flow of LCP melts in nanochannels. Whereas, studies on the flow of simple liquids and simple molecular structured polymer fluids at nano scale have made great progress [9–13]. Nikolai Priezjev et al. investigated the slip length in thin polymer films subject to planar shear using MD simulations [9]. Galea et al. presented a systematic study on the effect of surface roughness on the slipping boundary condition of shear flow with atomic scale MD, where the investigated fluid was simple LJ liquid [10]. They found that the fluid–solid slip length exhibited nonmonotonic behavior as the solid structure was varied from smooth to rough slip occurred for both smooth and rough surfaces. Jabbarzadeh et al. examined the effect of the wall roughness on the boundary condition and rheological properties of thin liquid films of alkanes [11]. The results showed that as the period of roughness increased, the degree of slippage on the wall also increased, while for relatively shorter molecules the amount of the slippage could be drastically reduced as the roughness amplitudes increased. Moreover, it was concluded that there was a dramatic effect of the wall roughness on the fluid viscosity. The above literatures [9–13] show that the solid surface roughness has great impact on the fluid–solid boundary conditions and the rheological properties of nanoflow. They also show the different flow behaviors of molecular fluids such as polymeric fluids and fluids of alkane molecules, and simple atomic fluids under the effect of the surface roughness at nano scale.

In this paper, we will investigate the nano flow of semi-flexible main chain LCP melt using a new MD model called GB-spring-bead model, which makes the speed of simulation 10 times faster than that of the GB/LJ model. The higher simulation speed has enabled a much more detailed micro flow investigation. Effects of roughness, such as period and amplitude of serrations, on the flowability of nano flow will be analyzed.

2. Computational models

In this study, the monomer unit of the thermotropic semi-flexible main chain LCP called LC main chain polyester PE1/*n* is

$$(\text{–COO–C}_6\text{H}_4\text{–COO–C}_6\text{H}_4\text{–COO–C}_6\text{H}_4\text{–COO–(CH}_2)_n\text{–})_m \tag{1}$$

where, typically $5 \le n \le 10$. This molecular structure is described by the GB-spring-bead model (Fig. 1), where all mesogenic elements of the molecule are described by Gay-Berne (GB) units whose interactions are given by modified GB

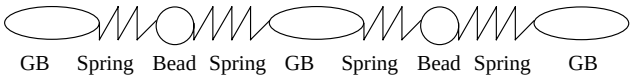

Fig. 1. GB-spring-bead model that represents two units of a LCP molecular chain.

potential [14]:

$$\begin{aligned} V_{\text{GB}} =& 4\varepsilon_0^{\text{GB}}[\varepsilon^{\prime\prime\text{GB}}(\boldsymbol{u}_i,\boldsymbol{u}_j)]^{\nu}[\varepsilon^{\prime\text{GB}}(\boldsymbol{u}_i,\boldsymbol{u}_j,\hat{\boldsymbol{r}}_{ij})]^{\mu} \\ &\times\left[\left(\frac{\sigma_0^{\text{GB}}}{r_{ij}-\sigma^{\text{GB}}(\boldsymbol{u}_i,\boldsymbol{u}_j,\hat{\boldsymbol{r}}_{ij})+\sigma_0^{\text{GB}}}\right)^{12}\right. \\ &\left.-\left(\frac{\sigma_0^{\text{GB}}}{r_{ij}-\sigma^{\text{GB}}(\boldsymbol{u}_i,\boldsymbol{u}_j,\hat{\boldsymbol{r}}_{ij})+\sigma_0^{\text{GB}}}\right)^{6}\right], \end{aligned} \tag{2}$$

where, $\boldsymbol{u}_i$ and $\boldsymbol{u}_j$ are unit vectors along the GB molecule long axes, $\hat{\boldsymbol{r}}_{ij} = r_{ij}/r_{ij}$ is the separation unit vector between particle i and j. The distance function σ^{GB} takes the following form

$$\begin{aligned} &\sigma^{\text{GB}}(\boldsymbol{u}_i,\boldsymbol{u}_j,\hat{\boldsymbol{r}}_{ij}) \\ &= \sigma_0^{\text{GB}}\left\{1-\frac{\chi}{2}\left[\frac{(\hat{\boldsymbol{r}}_{ij}\cdot\boldsymbol{u}_i+\hat{\boldsymbol{r}}_{ij}\cdot\boldsymbol{u}_j)^2}{1+\chi(\boldsymbol{u}_i\cdot\boldsymbol{u}_j)}+\frac{(\hat{\boldsymbol{r}}_{ij}\cdot\boldsymbol{u}_i-\hat{\boldsymbol{r}}_{ij}\cdot\boldsymbol{u}_j)^2}{1-\chi(\boldsymbol{u}_i\cdot\boldsymbol{u}_j)}\right]\right\}^{-1/2} \end{aligned} \tag{3}$$

where $\chi=(k^2-1)/(k^2+1)$ and $k=\sigma_{\text{ee}}/\sigma_{\text{ss}}\cdot\sigma_{\text{ee}}$ is the molecular length along the main symmetry axis and σ_{ss} is the cross-section diameter of the molecule. Here, the length to breadth ratio is set as $\sigma_{\text{ee}}/\sigma_{\text{ss}}=3$.

The orientation dependent well depths $\varepsilon^{\prime\text{GB}}$ and $\varepsilon^{\prime\prime\text{GB}}$ are given by Eq. (4)

$$\varepsilon^{\prime\text{GB}}(\boldsymbol{u}_i,\boldsymbol{u}_j,\hat{\boldsymbol{r}}_{ij}) = 1-\frac{\chi'}{2}\left[\frac{(\hat{\boldsymbol{r}}_{ij}\cdot\boldsymbol{u}_i+\hat{\boldsymbol{r}}_{ij}\cdot\boldsymbol{u}_j)^2}{1+\chi'(\boldsymbol{u}_i\cdot\boldsymbol{u}_j)}+\frac{(\hat{\boldsymbol{r}}_{ij}\cdot\boldsymbol{u}_i-\hat{\boldsymbol{r}}_{ij}\cdot\boldsymbol{u}_j)^2}{1-\chi'(\boldsymbol{u}_i\cdot\boldsymbol{u}_j)}\right] \tag{4a}$$

$$\varepsilon^{\prime\prime\text{GB}}(\boldsymbol{u}_i,\boldsymbol{u}_j) = [1-\chi^2(\boldsymbol{u}_i\cdot\boldsymbol{u}_j)^2]^{-1/2} \tag{4b}$$

where $\chi' = (k'^{1/\mu}-1)/(k'^{1/\mu}+1)$ and $k'=\varepsilon_{\text{ss}}/\varepsilon_{\text{ee}}\cdot\varepsilon_{\text{ss}}$ is the minimum of the potential for a pair of parallel molecules placed side-by-side ($\hat{\boldsymbol{r}}_{ij}\cdot\boldsymbol{u}_i=\hat{\boldsymbol{r}}_{ij}\cdot\boldsymbol{u}_j=0$) and ε_{ee} is the minimum for a pair of parallel molecules placed end-to-end ($\hat{\boldsymbol{r}}_{ij}\cdot\boldsymbol{u}_i=\hat{\boldsymbol{r}}_{ij}\cdot\boldsymbol{u}_j=1$). Here, $\varepsilon_{\text{ss}}/\varepsilon_{\text{ee}}$ is assumed to be 5. Meanwhile, the values $\sigma_0^{\text{GB}}=0.4721$ nm, $\varepsilon_0^{\text{GB}}/k_{\text{b}}=406.51$ K, $\mu=2$ and $\nu=1$ were used in our simulation. The values of all parameters in the GB potential are given in the same way as Ref. [7].

In the GB-spring-bead model, the flexible spacers between rigid units are modeled by two springs and a bead in the middle with each spring connecting to its adjacent GB unit, and a mass compensation coefficient W_1, a strength compensation coefficient W_2 and the nonlinear spring potential are used. The expressions of the coefficients and potential are shown in Eqs. (5) and (6), respectively.

$$W_1 = \frac{(n_{\text{s}}^3-n_{\text{s}}-0.5)}{n_{\text{s}}^2}, \qquad W_2 = \frac{4(n_{\text{s}}-3)}{n_{\text{s}}} \tag{5}$$

Here n_s is regarded as the number of flexible spacers (the flexible spacer length).

$$V_{sp} = -0.5K_s(r_{si} - r_{s0})^2 + 0.5K_a f_s(\alpha_i - \alpha_0)^2 + 0.5K_t(\alpha_{ijk} - \alpha_0)^2 \quad (6)$$

where r_{si} is the distance from the center of the LJ site to the adjacent ending point of the GB site, α_i is the angle between the long axis of the GB site and the separation from the center of the GB site to the center of the LJ site and α_{ijk} is the angle between two displacements from the LJ site to two adjacent GB sites. The energy parameters K_s, K_a, K_t assumed values of 3.6129×10^{-20}, 8.654×10^{-19}, 8.654×10^{-19} J, respectively, in this work. The equilibrium angle is defined as $\alpha_0 = 180°$. The equilibrium distance is given by

$$r_{s0} = \frac{0.5(3n_s - 5.0)}{2.0}. \quad (7)$$

This equation is used to change the corresponding length of a molecular chain with different number of flexible spacers in this model. The energy coefficient f_s is related to the number of flexible spacers by the equation

$$f_s = \frac{2(f_I + 1.0)}{n_s}, \quad (8)$$

where, f_I is equal to the integer value of $n_s/2.0$.

The interaction energy between two beads is given by the standard shifted 12:6 LJ potential multiplied by the strength compensation coefficient W_2, as shown in Eq. (9).

$$V_{LJ} = W_2\left\{4\varepsilon_0^{LJ}\left[\left(\frac{\sigma_0^{LJ}}{r_{ij}}\right)^{12} - \left(\frac{\sigma_0^{LJ}}{r_{ij}}\right)^{6}\right] + \varepsilon_0^{LJ}\right\}, \quad r_{ij} <= r_c,\ r_c = 2^{1/6}\sigma_0^{LJ} \quad (9)$$

where, σ_0^{LJ} and ε_0^{LJ}/k_b equal 0.3923 nm and 72 K, the same as Ref. [7].

The interaction energy between a GB unit and a bead is described by the generalized potential from the work of Cleaver et al. [15] multiplied by the strength compensation coefficient W_2, as shown in Eq. (10).

$$V_{LJ/GB} = 4W_2\varepsilon^{LJ/GB}(\hat{\boldsymbol{u}}_j,\hat{\boldsymbol{r}}_{ij})\left[\left(\frac{\sigma_0^{LJ/GB}}{r_{ij} - \sigma^{LJ/GB}(\hat{\boldsymbol{u}}_j,\hat{\boldsymbol{r}}_{ij}) + \sigma_0^{LJ/GB}}\right)^{12} - \left(\frac{\sigma_0^{LJ/GB}}{r_{ij} - \sigma^{LJ/GB}(\hat{\boldsymbol{u}}_j,\hat{\boldsymbol{r}}_{ij}) + \sigma_0^{LJ/GB}}\right)^{6}\right] \quad (10)$$

where, $\sigma^{LJ/GB}$ and $\varepsilon^{LJ/GB}$ are given, respectively, by Eqs. (20) and (37) of Ref. [15]. Values of $\sigma_0^{LJ/GB} = 0.4117$ nm and $\varepsilon_0^{LJ/GB}/k_b = 17,108$ K were used in the same way as Ref. [1].

The LCP melt is assumed to be subject to planar shears in a nanometer channel by translating the upper wall and the lower wall in opposite directions. The two walls of the shear cell each consists of 1920 atoms distributed between two (111) planes of a fcc (face-centered-cubic) lattice. The configuration of LCP melt flowing in the nanochannel is shown in Fig. 2. Where,

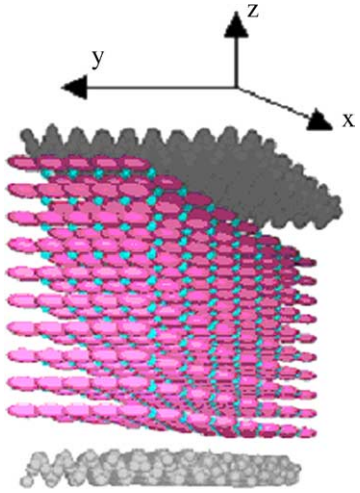

Fig. 2. The configuration of LCP shear flow in the nanochannel.

x-axis is the direction of shear, z-axis is perpendicular to the xy plane. The positions of the particles on the wall in the direction z are displaced by Δz given by:

$$\Delta z = \begin{cases} \frac{2A}{P}(x - aP) & x - aP \le \frac{P}{2} \\ \frac{2A}{P}((a+1)P - x) & x - aP > \frac{P}{2} \end{cases} \quad (11)$$

where, A and P, characterizing the roughness, are the amplitude and period of the serrated wall, respectively (Fig. 3) and a = integer(x/p). Each atom on the wall is attached to its lattice position by a stiff spring. The potential of spring is expressed by $\phi_s = 0.5\ k_w R^2$, where, k_w is the spring stiffness equal to 6000 $\varepsilon_0^{LJ}\sigma_0^{LJ^2}$, and R is the distance of the atom from its lattice site. The interaction between beads and atoms on the wall is modeled as shifted LJ potential with the energy scale $\varepsilon_w = 3\varepsilon_0^{LJ}$ and the length scale $\sigma_w = \sigma_0^{LJ}$. Here, ε_0^{LJ} and σ_0^{LJ} are the energy and length parameter in the potential between a pair of beads (as seen in Eq. (9)). The interactions between GB units and atoms on the wall are given by the generalized potential with the energy scale $\varepsilon_{ws} = 0.55\varepsilon_0^{GB}$ and the length scale $\sigma_{ws} = 0.87\sigma_0^{GB}$, where, ε_0^{GB} and σ_0^{GB} are the energy and length parameter in the GB potential (as seen in Eq. (2)). The interaction energy between the wall atom and the fluid molecule interaction sites is close to a typical surface energy of metals (for the gold surface, ε_{wg}/k_b is about 220 K [16]). The entire simulation cell (xyz) measures $14.0\times6.0\times12.8$ nm^3 and the LCP melt is confined in a gap of the width $h = 12.8 - 2A$ nm. Periodic boundary conditions are imposed in the $\hat{x}$ and $\hat{y}$ directions. For all the simulations here, a constant shear rate $\dot{\gamma} = 10^{11}$ s^{-1} is used.

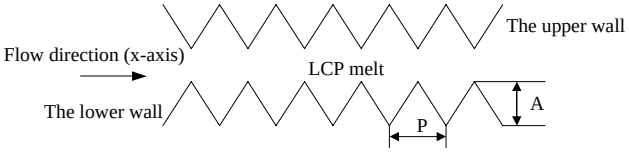

Fig. 3. The scheme of the LCP shear flow between the two serrated walls.

3. Simulation algorithms

The simulation system includes 50 LCP molecular chains with the degree of polymerization $M=8$. The initial configuration of LCP melt starts from a low molecular density in an all-trans configuration aligned parallel to the x-axis of the simulation box. Polymer molecules are arranged with random centers of mass vectors and all particle velocities are taken from a Maxwell–Bolzmann distributions. The equations of motions are integrated using a leap-frog Verlet algorithm [17]. Initially, calculations for only LCP molecules to form the liquid crystalline phase (the wall particles are excluded temporarily) are carried out. Then ensemble (NVT) simulations of shear flow in constant temperature (at $T=350$ K) start, where Gaussian thermostat [18] is used in all three directions. The time step used in the simulation is 4 fs. The equilibrium run takes 1×10^7 time steps followed by another 2×10^7 time steps for collecting results.

To investigate the rheology of LCP melt between the walls with different surface roughness parameters, Iriving–Kirkwood relation [19] is used for computing the stress tensor components by the following form:

$$\sigma_{\alpha\beta} = -\frac{1}{V}\left\langle \sum_i^N m_i v_{i\alpha} v_{i\beta} + \sum_i^N \sum_{j>i}^N r_{ij\alpha} F_{ij\beta} \right\rangle, \quad \alpha,\beta = x,y,z \tag{12}$$

where, m_i is the atomic mass, $v_{i\alpha}$, $v_{i\beta}$ are the peculiar velocity components of particle i in the α and β directions, $r_{ij\alpha}$ is the α component of the distance vector between particle i and j and $F_{ij\beta}$ is the β component of the force exerted on particle i by particle j. For velocity in the flow direction, the mean flow velocity is subtracted. Hence, the shear stress can be rewritten as

$$\sigma_{xz} = -\frac{1}{V}\left\langle \sum_i^N m_i v_{iz}[v_{ix} - \bar{U}_{x,i}] + \sum_i^N \sum_{j>i}^N r_{ijx} F_{ijz} \right\rangle, \tag{13}$$

where, $\bar{U}_{x,i}$ is the average flow velocity at the position of particle i and is evaluated using Eqs. (9)–(11) in Ref. [19]. Moreover, in this paper, the measurement of the shear viscosity takes the constitutive equation related to the shear stress:

$$\eta = \sigma_{xz}\dot{\gamma}, \tag{14}$$

where, $\dot{\gamma}$ is the shear rate, η is the average over the whole width of the gap. During the production run, The orientational ordering of the mesogenic units is monitored by Eqs. (15) and (16).

$$S_2 = \langle P_2(\cos\theta)\rangle = \left\langle \frac{3}{2\cos^2\theta} - \frac{1}{2} \right\rangle \tag{15}$$

where, θ is the angle between the long axis of the GB ellipsoid and the average orientation of the sample, which is defined by the director $\boldsymbol{n}$. In this simulation, S_2 is associated with the largest eigenvalue λ_+ obtained through the diagonalization of the ordering tensor,

$$Q_{\alpha\phi} = \frac{1}{N_{\mathrm{GB}}}\sum_{i=1}^{N_{\mathrm{GB}}} \frac{3}{2} u_{i\alpha} u_{i\beta} - \frac{1}{2}\delta_{\alpha\beta}, \quad \alpha\beta = x,y,z. \tag{16}$$

where, $u_{i\alpha}$, $u_{i\beta}$ are the components of the orientation unit vectors along molecular long axes of GB particle i. The eigenvector associated with λ_+ provides the director $\boldsymbol{n}$ for describing the average direction of alignment for GB particles.

4. Results and discussions

Before the LCP melt flows into the nanochannel, the melting process is carried out. In other words during initial MD simulation, firstly the LCP is heated till it is completely molten and forms isotropic phase under high system temperature ($T=500$ K). Then the molten LCP keeps relaxing as the system temperature decreases gradually. When the system temperature is reduced to 350 K, the LCP molecules exhibit alignments in order (as shown in Fig. 4), which implies the LCP melt forms a liquid crystalline phase, a nematic phase. This can be confirmed by analyzing the radial and second-rank orientational distribution functions of GB particles (Fig. 5). As shown in Fig. 5(a), the curve of $g(r)$ forms two peaks and troughs at the beginning and then tends to the constant value of 1.0 at larger separations (r), which indicates there are positional correlation between neighboring sites. But these peaks do not bifurcate and oscillate, suggesting the liquid crystalline phase is nematic but not smectic. In Fig. 5(b), the function $g_2(r)$ shows two peaks at smaller r, the principle peak reflects some short-range side-by-side ordering and the smaller peak indicates strong orientational correlation between GB particles within the liquid crystalline molecules. The values of the function $g_2(r)$ at larger separations (r) in the liquid crystalline phase approach the constant value of 0.38 that equals approximately to the square of the relative orientational order parameter (statistically measured $S_2\approx0.62$), which agrees with those in the previous work [1]. Hence, it is convinced that the current LCP melt at $T=350$ K stays in the nematic phase.

After the LCP melt forms liquid crystalline phase, the NVE ensemble is performed to collect the equilibrated state points. Then, the collected state points are regarded as the new configuration of the LCP melt on which the shear flow field and the surface wall forces are exerted. With the developed simulation programs, effects of serrations amplitude (A) and

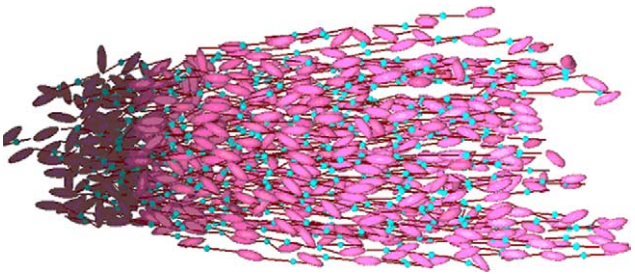

Fig. 4. The configuration of the LCP molecules with $M=8$, $n_s=6$ at the system temperature $T=350$ K.

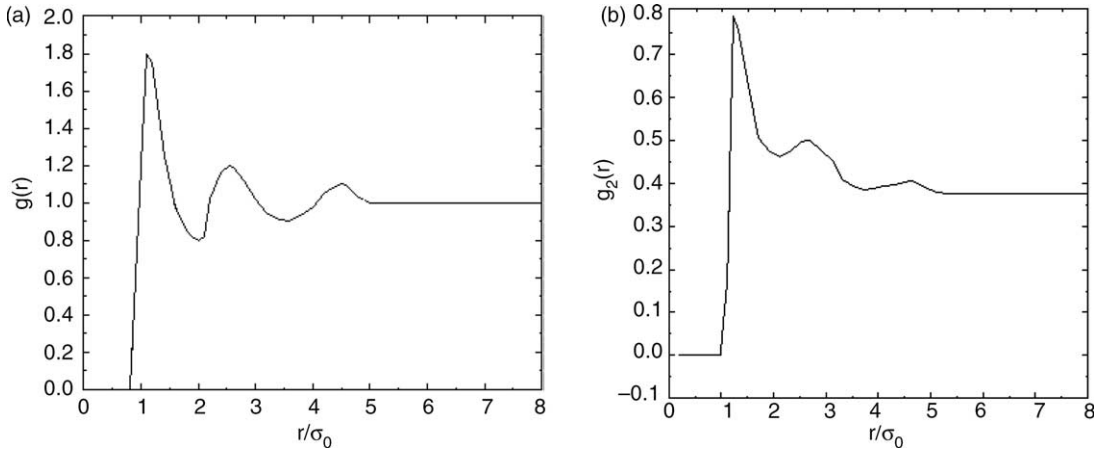

Fig. 5. (a) The radial distribution function $g(r)$ of GB particles at $T=350$ K; (b) the second-rank orientational distribution function $g_2(r)$ of GB particles at $T=350$ K.

period (P) (on the wall surface) on the rheology and structural properties of LCP melts, are examined (see Sections 4.1 and 4.2). The average shear viscosity and average orientational order parameter at different amplitudes and periods are calculated. Results are shown in Figs. 6–9.

4.1. The effect of roughness amplitude (A) on the LCP melt

One of the most important factors of surface topology is the amplitude of asperities. In the serrated wall model the amplitude is expressed by A. The PE/n melt in the liquid crystalline phase is assumed to flow into the serrated nano channel under a constant shear rate. The system temperature is kept at 350 K and the serration period (P) is set at a constant value of 1.3471 nm. The shear viscosity of the LCP melt film for different values of A is depicted in Fig. 6. It shows the shear viscosity increases nonlinearly when the value of A goes up from 0.1 to 1.2 nm. The increasing speed is lower when the value of A is between 0.1 and 1.0 nm (from 1.3535 mPas) at $A=0.1$ nm to 2.0045 mPas at $A=1.0$ nm), where the shear viscosities for the serration amplitude A between 0.1 and 0.6 nm are close to those of alkane under similar conditions (as shown in Fig. 15 of Ref. [11]). However, when the value of A is greater than 1.0 nm, the shear viscosity soars up drastically, reaching a high value of 3.8336 mPas at $A=1.2$ nm.

The reason that the shear viscosities of the LCP melt are so low when A is between 0.1 and 1.0 nm can be explained by analyzing the relationship between the orientational order parameter and the amplitude (Fig. 7). When the value of A is between 0.1 and 1.0 nm, the orientational order parameter s_2 is still very high (≥ 0.5), which indicates that LCP melt is in the liquid crystalline phase. In other words, the liquid crystalline phase of the LCP melt is not seriously affected by the interface interactions. It can be seen that the formation of the liquid crystalline phase can greatly reduce the viscosity of the nano LCP melt flow and improve its flowability, which accordingly might make the polymer processing at nano scale much easier.

The abrupt increase of viscosity when A reaches 1.0 nm is also related to the change of the orientational structure in the LCP melt. As shown in Fig. 7, when the value of A is larger than 1.0 nm, the value of S_2 falls down promptly (reaching the value of 0.315), which indicates the LCP melt is no longer in liquid crystalline phase and a phase transition has occurred. This is probably because, on the one hand, when the amplitude

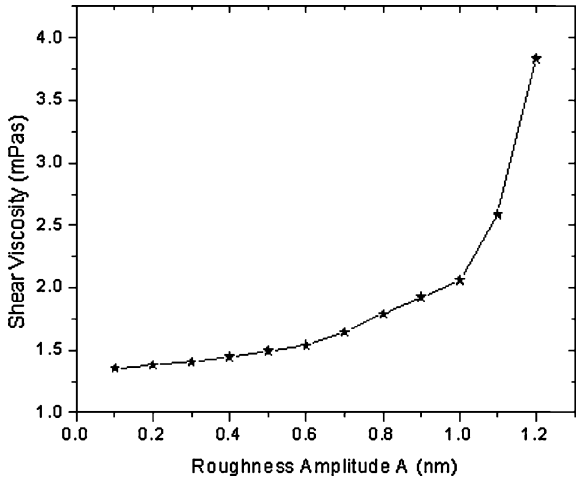

Fig. 6. The shear viscosity against the amplitude ($P=1.3471$ nm, $\dot{\gamma}=10^{11}$ s^{-1}).

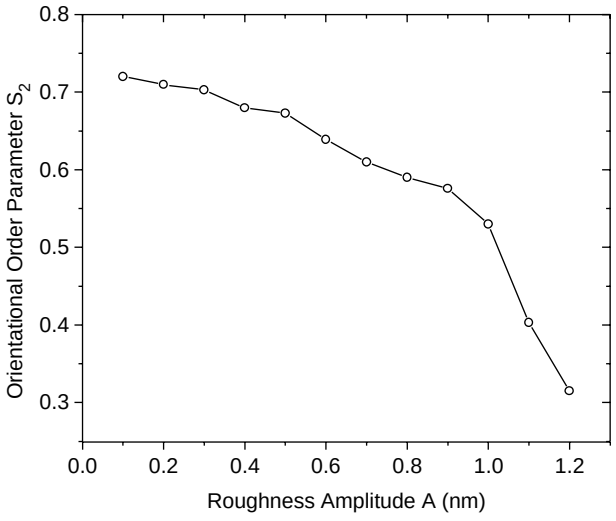

Fig. 7. The orientational order parameter against the amplitude ($P=1.3471$ nm, $\dot{\gamma}=10^{11}$ s^{-1}).

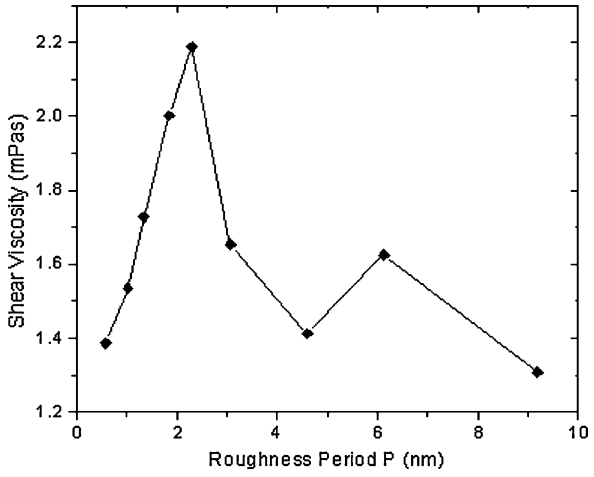

Fig. 8. The shear viscosity against the period ($A=0.5$ nm, $\dot{\gamma}=10^{11}$ s^{-1}).

A increases the gap width ($h=12.8-2A$ nm) becomes narrower, and on the other hand, the number of total interacting particles between the wall and the LCP melt becomes relatively larger and the binding effect of the wall on the LCP molecules is stronger. The binding effect makes some parts of LCP molecular chains being trapped in the deep valleys of the serrated wall. These molecules even cannot be released by the interactions with neighboring chains. Consequently, the molecular chains entangle with each other, forming a typical isotropic phase (entanglements destruct nematic state), and the shear viscosity of the LCP melt is 3.8335 nearly three times of that in the liquid crystalline phase (1.3535). It is obvious that the amplitude of wall roughness has a profound effect on flow features of nano-LCP melts.

4.2. The effect of roughness period (P) on the LCP melt

To study the effect of serration period on the nano-LCP melt, the amplitude of the serration is kept constant at $A=0.5$ nm (about equal to $1.0\sigma_{GB}$). The dependences of the shear viscosity and the orientational order parameter on the serration periods are shown in Figs. 8 and 9, respectively. Fig. 8 shows that the shear viscosity of the LCP melt is the largest ($\eta=2.1863$ mPas) when the period is 2.2986 nm and there is a small jump at $p=6.13$ nm. These are mainly caused by the periodic molecular structures of LCPs. When the period size is multiple times of the distance between GB units, the chances of serration tips and GB units 'contact' each other become larger, and the higher interactions between serration tips and GB units makes roughness effects more obvious. However, these effects are not so apparent compared with those of amplitudes (Figs. 6 and 7). The relation between the orientational order parameter and the sizes of the period (as shown in Fig. 9) is similar to that of the shear viscosity, which exhibits no dramatic changes (values are between 0.5 and 0.66), indicating there are no phase transitions caused by the change of period dimensions. The relations between shear viscosity and roughness period resulting from our simulations are roughly similar to that of hexadecane molecules [11], where it had been suggested that the period P had little or no effect on the film properties except that when it was comparable with the size of the molecules. (Here the length of LCP molecular chains is around 9.3 nm).

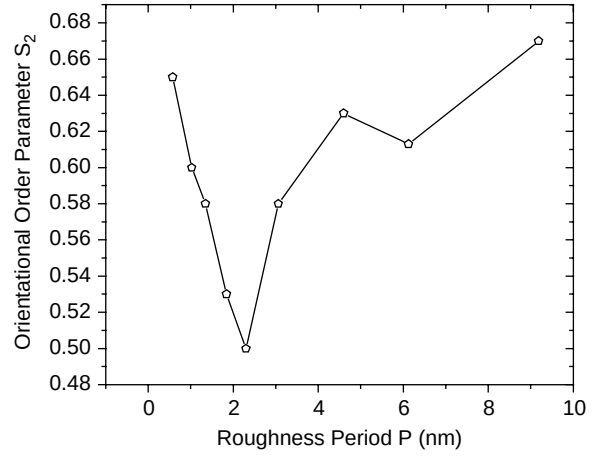

Fig. 9. The orientational order parameter against the period ($A=0.5$ nm, $\dot{\gamma}=10^{11}$ s^{-1}).

5. Conclusions

In this paper, the effects of wall roughness on the rheological and structural properties of the nano-melt flow of LCP have been studied for the first time using MD simulations. Results show that the asperity amplitude has a profound impact on the nano LCP flow. When the shear rate is 10^{11} s^{-1} and the serration amplitude is 1.2 nm, the shear viscosity increases sharply with serration amplitudes. This is because there is a phase transition from the liquid crystalline phase to the isotropic phase under the influence of the asperities. Phenomena observed in our study show distinctions of LCP melt from other polymer materials when flowing in nanoscaled channels that wall roughness amplitude can affect the fluid viscosity dramatically. In the mean time, results also suggest that the effect of roughness period is not so obvious as that of amplitude, which approximately agrees with phenomena observed for other low-weight molecular materials. To thoroughly understand the rheology of nanoflow of LCP melt, further investigations are needed, which includes the phenomena of slippage, effects of shear rates and surface energy on the flow etc.

Acknowledgements

The work described in this paper was supported by a fund from the Hong Kong Research Grant Council (PolyU 5314/05E).

References

[1] Yung KL, He Lan, Xu Yan, Shen YW. Polymer 2005;46:11881.
[2] Duska, JJ, Field, ND, Scardigila, F. Polym process Soc Conf; (Montreal, 1987).
[3] Zulle B, Demarmels C, J G, Plummer HH. Polymer 1993;34:3628.
[4] Khennache O, Kamal MR. SPE ANTEC Tech, papers 1989;35:1721.

[5] Muataz S, Al-Barwani MP. Phys Rev E 2000;62:6706.
[6] Mark R. Wilson. J Chem Phys 1997;107:20.
[7] Lyulin AV, Al-Barwani MS, Allen MP. Macromolecules 1998;31:4626.
[8] Melker AI, Efleev AN. J Macromol Sci Phys B 1999;38:769.
[9] Priezjev NV, Troian SM. Phys Rev Letts 2004;92(1):018302.
[10] Galea TM, Attard Phil. Langmuir 2004;20:3477.
[11] Jabbarzadeh A, Atkinson JD, Tanner RI. Phys Rev E 2000;61:690.
[12] Nagayama Gyoko, Cheng Ping. Int J Heat Mass Transfer 2004;47:501.
[13] Markvoort AJ, Hilbers PAJ. Phys Rev E 2005;71:066702.
[14] Gay JG, Berne BJ. J Chem Phys 1981;74:3316.
[15] Cleaver DJ, Care CM, Allen MP, Neal MP. Phys Rev E 1996;53:1.
[16] Xia TK, Ouyang J, Ribarsky MW, Landman U. Phys Rev Lett 1992;69:1967.
[17] Allen MP, Tildesley DJ. Comput Simul Liq. New York: Oxford University Press; 1987 p. 78.
[18] Jabbarzadeh A, Atkinson JD, Tanner RI. Comput Phys Commun 1997; 107:123.
[19] Jabbarzadeh A, Atkinson JD, Tanner RI. J Non-Newtonian Fluid Mech 1998;77:53.